Layer-by-Layer Self-Assembled Single-Walled Carbon Nanotubes Based Ion-Sensitive Conductometric Glucose Biosensors

Dongjin Lee and Tianhong Cui, *Senior Member, IEEE*

***Abstract*—We present ion-sensitive conductometric glucose sensors prepared by layer-by-layer (LbL) nano self-assembly of single-walled carbon nanotube (SWNT) and enzyme glucose oxidase (GOx). The carboxylated SWNT and GOx are self-assembled alternatively with a positively charged polyelectrolyte, poly(diallyldimethylammonium chloride, PDDA). Quartz crystal microbalance (QCM) study and Fourier transform infrared (FTIR) spectroscopy demonstrate GOx is negatively charged, and it is possible to successively construct multilayer alternatively with PDDA. SWNT multilayer shows pH-dependent conductance at different pH buffer solutions, which decreases exponentially with an increase in pH. The concentration of glucose is electronically characterized based on the fact that hydrogen ions from glucose oxidation with the aid of GOx change the local pH value in the vicinity of SWNT multilayer thin-film, thereby yielding higher conductance. The overall sensitivity is 10.8 $\mu\mathrm{A}/\mathrm{mM}$ and the resolution of device fabricated is 1 pM at the bias voltage of 0.6 V. The LbL assembled SWNT multilayer is proven to be versatile for sensing biochemical reactions with many other enzyme systems.**

***Index Terms*—Fourier transform infrared (FTIR), glucose oxidase (GOx), glucose sensor, layer-by-layer (LbL) assembly, quartz crystal microbalance (QCM), single-walled carbon nanotube (SWNT).**

I. Introduction

SINCE the discovery by Iijima [1] in 1991, carbon nanotubes (CNT) have been of great interest in many research and development areas due to the extraordinary mechanical and unique electronic property with the excellent thermal and chemical stability [2]. CNT becomes one of the promising functional materials for applications mostly to chemical [3] and biological sensors [4], actuators [5], nanoelectronics [6], nanoelectromechanical systems (NEMS) [7], and microscopy [8], etc.

The studies of the electrochemical property of CNTs substantially make them very useful for biosensing applications [9]. CNT-based biosensors reported detected protein [10], DNA [11], immunoglobulin [12], neurotransmitters [13] and other molecules [14] for the purpose of diagnostics in the presence or absence of bio-receptors, reacting specifically with target biomolecules.

The glucose sensors are in the forefront of recent advances in biosensors due to the high demand of diabetes diagnosis and the necessity of the monitoring glucose level in the fermentation process in the food industry. Most glucose sensors have been developed as an amperometric type, where electrons are transferred from the glucose to the modified metal electrode with or without the aid of glucose oxidase (GOx) as a catalyst. Emphasis has been placed on the surface modification of electrodes to increase the sensitivity and reduce the response time.

Among those, the surface modification by various functional nanomaterials has become the main stream of electrochemical sensors to exploit their novel properties. Multiwalled CNT (MWNT) modified glucose sensors showed higher sensitivity and longer stability than glassy carbon-based sensors [15]. As a further advance form, MWNTs were decorated with nanoparticles [16] and conducting polymers [17] to enhance the electrochemical property of CNTs themselves. Recently, combined with a facile layer-by-layer (LbL) self-assembly technique, CNT was deposited on the electrode surface to construct the glucose sensors alternated with GOx [18], gold nanoparticles [19], and both chitosan and GOx [20]. Other electrochemical glucose sensors are conductometric types based on ion-sensitive field effect transistors (ISFETs). Among those, nanomaterial-based glucose sensors were constructed using $\mathrm{SiO_2}$[21] and $\mathrm{MnO_2}$ nanoparticles [22] in combination with GOx as a gate electrode. Our group previously reported nanoparticle-based glucose ISFET sensors with $\mathrm{In_2O_3}$ as a semiconducting layer and $\mathrm{SiO_2}$ nanoparticles as a dielectric material [23].

To the best of our knowledge, however, there have not been LbL self-assembled thin-film planar conductometric glucose sensors. The planar devices are advantageous in that they can be used for continuous monitoring using the simplicity of the electronic detection and are low-cost due to the possibility of mass production [24]. Furthermore, it can be incorporated into implantable devices for possible *in-vivo* applications. In this paper, we describe a hydrogen ion-sensitive SWNT multilayer on which GOx enzymes were immobilized using a facile LbL assembly. The LbL assembled SWNT multilayer showed pH-dependent conductance, which decreases exponentially with increase in pH values due to protonation/deprotonation of a SWNT network. The pH changes induced in the process of

Manuscript received July 04, 2008; revised August 27, 2008; accepted August 27, 2008. Current version published March 04, 2009. This work is partially supported by the DARPA M/NEMS Science and Technology Fundamental Research Program through the Micro/Nano Fluidic Fundamental Focus (MF3) Center. The associate editor coordinating the review of this paper and approving it for publication was Prof. Evgeny Katz.

The authors are with the Department of Mechanical Engineering, University of Minnesota, Minneapolis, MN 55455 USA (e-mail: djlee@umn.edu; tcui@me.umn.edu).

Color versions of one or more of the figures in this paper are available online at http://ieeexplore.ieee.org.

Digital Object Identifier 10.1109/JSEN.2009.2014414

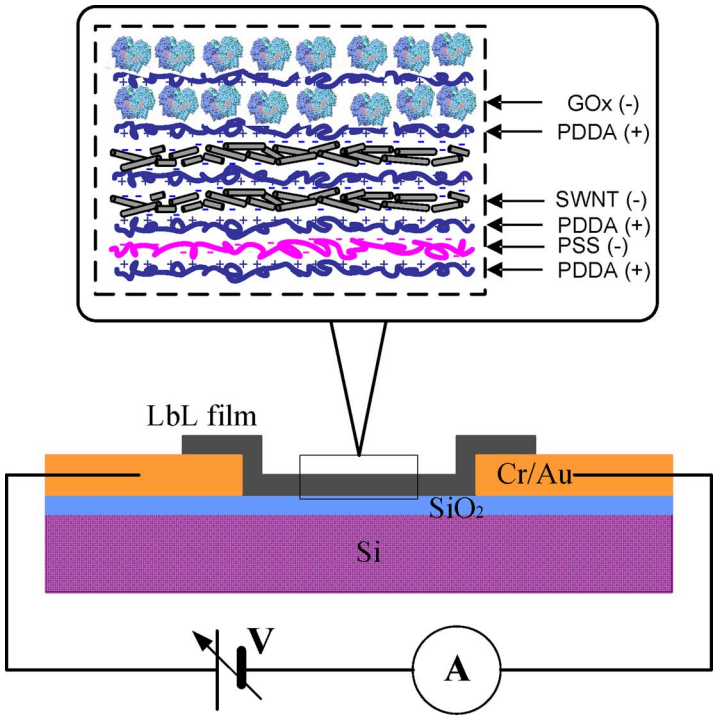

Fig. 1. Schematic diagram of the LbL assembled SWNT and GOx based glucose sensor along with the electronic testing scheme. Bias voltage is applied to source and drain electrodes with sample solution on top of LbL thin-film and the current is sampled.

glucose oxidation by the enzyme GOx cause the conductance changes of SWNT multilayer, resulting in the current changes flowing through the multilayer.

II. Experimental

A. Materials

SWNTs (1–2 nm in diameter, 50 μm in length) were chemically functionalized with 3:1 mixture of concentrated sulfuric (H_2SO_4) and nitric acid (HNO_3) at 110 °C for an hour, followed by membrane filtering with the pores of 0.22 μm to remove soot, metallic particles, and shorter CNTs. After several rinsing with deionized water (DIH_2O) until the pH approached to 5, the functionalized SWNTs were harvested and redispersed into DIH_2O with the aid of ultra-sonication for an hour. The SWNT solution was centrifugated at a speed of 5000 rpm (4500 g, Eppendorf centriguge 5804) for 20 min to eliminate longer CNTs, aggregates and bundles. Subsequently, the supernatant was carefully decanted and precipitated, aggregates and bundles were abandoned. The final concentration of a SWNT solution was about 0.06 wt%.

GOx (50 ku/g) from Aspergillus niger was purchased from Aldrich. The concentration of GOx solution used in this study was 1 mg/mL into 1X phosphate buffered solution (PBS, pH7.2). Polyelectrolytes used for LbL assembly were poly(diallyldimethyammonium chloride, PDDA, $M_w = 200 \sim 350$ k, Aldrich) and poly(stylenesulfonate, PSS, $M_w = 70$ k, Aldrich). The concentration of PDDA and PSS used was 1.4 wt% and 0.3 wt%, respectively, with 0.5 M sodium chloride (NaCl) for better surface coverage.

B. Device Fabrication

A standard 4 inch silicon (Si) wafer with silicon dioxide (SiO_2) 2 μm thick was cleaned in a piranha solution (3:1H_2SO_4:H_2O_2) at 120 °C for 15 minutes, rinsed thoroughly with a copious amount of DIH_2O, and dried with a nitrogen (N_2) stream. Chromium (Cr, 100 nm) and gold (Au, 200 nm) were electron-beam evaporated onto the Si/SiO_2 substrate, and patterned for source-drain electrodes using photolithography. Another lithographic technique was used to fabricate a window area on which the LbL film was assembled and to protect the measuring pad from the adsorption of CNTs. After developing photoresist, oxygen (O_2) plasma was used to remove the residual photoresist completely in the opening window at a power of 100 W for 1 minute with O_2 flow rate of 100 sccm as well as to make the surface hydrophilic, which is essential for subsequent LbL assembly.

Two bi-layers of (PDDA/PSS) were self-assembled as a precursor layer on the patterned substrate for charge enhancement, followed by the assembly of $(PDDA/SWNT)_5$ as a transducer material. Following SWNT multilayer, three bi-layers of (PDDA/GOx) were LbL-assembled as bio-receptors. The dipping time used here was 10 min for polyelectrolytes and GOx, and 15 min for SWNT. The schematic diagram of the LbL assembled SWNT and GOx based glucose sensor is shown in Fig. 1. There are three different layers, $(PDDA/PSS)_2$ as a precursor layer for the charge enhancement, $(PDDA/SWNT)_5$ as an electrochemical transducer, and $(PDDA/GOx)_3$ as a bio-receptor.

C. Quartz Crystal Microbalance (QCM) Measurement

The whole process for LbL assembly of both SWNT transducing layers and GOx bio-receptors was monitored by quartz crystal microbalance (RQCM, Maxtek Inc.) at room temperature. The used crystal is the AT cut 9 MHz with the active oscillation area of 0.34 cm^2.

First of all, two bi-layers of (PDDA/PSS) were deposited on the 9 MHz crystal for the charge enhancement of the crystal surface, followed by 5 bi-layers of (PDDA/SWNT) as the transducer materials. Finally, GOx was assembled on the SWNT layer alternatively with PDDA. After every layer, thorough washing with $\mathrm{DIH_2O}$ was performed to prevent precipitations, which hamper uniform coating of subsequent materials, followed by a nitrogen ($\mathrm{N_2}$) drying. This QCM characterization simulated the exact process of the fabrication of glucose sensors. Frequency shift after the assembly of each layer was monitored and recorded with the sampling frequency of 1.25 kHz.

D. Fourier Transform Infrared (FTIR) Spectroscopy

A silicon wafer with silicon dioxide 2 $\mu\mathrm{m}$ thick was cleaned with piranha as aforementioned to remove the organic contaminants. To demonstrate the assembly of GOx onto PDDA terminated surface, GOx was assembled with an alternative layer of PDDA after depositing two bi-layers of (PDDA/PSS). The reflective FTIR (Nicolet Magna IR 750) spectroscopy was used to characterize PDDA, (PDDA/PSS), and $(\mathrm{PDDA/PSS})_2(\mathrm{PDDA/GOx})$ surfaces with the background of the bare $\mathrm{SiO_2}$ surface. FTIR spectra were obtained in the mid-infrared (MIR) region, 4000–1000 cm^{-1} by an average of 500 scans with a spectral resolution of 2 cm^{-1}.

E. Electronic Characterization

The fabricated sensors were dipped into at different pH buffer solutions (mixture of $\mathrm{KH_2PO_4}$ and $\mathrm{K_2HPO_4}$) with buffer strength of 50 mM to demonstrate pH-dependent conductance behavior of LbL assembled SWNT transducing layers. The resistance of the device was recorded with the time using data logging system (Agilent 34970A Data acquisition/switch unit) and was converted into the conductance. In addition, I-V characteristics was measured using semiconductor parameter analyzer (HP 4156A) at different pH buffer solutions over the range of biochemical reactions. For glucose detection, three different kinds of devices (the ones only with GOx, the ones only with SWNT, and the ones with both SWNT and GOx) were prepared to show that the combination of SWNT and GOx plays a key role of glucose sensing. Furthermore, devices were characterized using parameter analyzer at different glucose concentration on the physiological ranges (2–10 mM) dissolved in phosphate buffered saline (PBS), as well as low concentration to evaluate the performance of the fabricated sensors. The characterized devices were stored at 4 °C for 15 days and recharacterized to investigate the stability of devices.

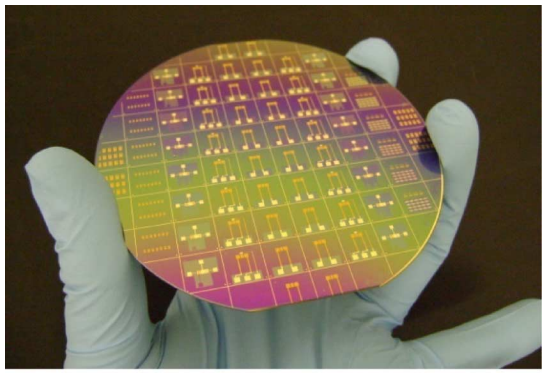

(a)

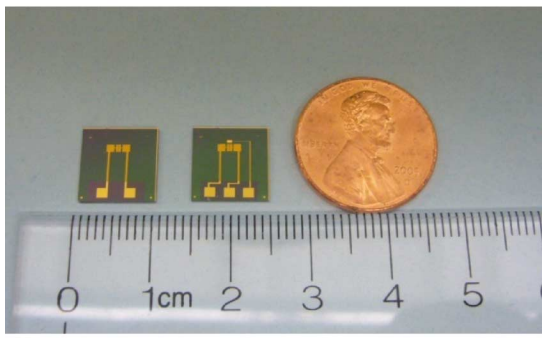

(b)

Fig. 2. The fabricated conductometric glucose sensor: (a) a standard 4 inch wafer scale fabrication and (b) individual chips.

III. Results and Discussion

The fabricated devices on the standard 4 inch wafer and individual chips are shown in Fig. 2, where only two terminal devices are used. To characterize the SWNT terminated surface with Scanning electron microscope (SEM, Jeol 6500), the surface of $(\mathrm{PDDA/PSS})_2(\mathrm{PDDA/SWNT})_5$ were sputter-coated with platinum 50 Å thick. SEM images were obtained at an acceleration voltage of 10 kV, as shown in Fig. 3. The individual SWNTs as well as their bundles are observed and they form a random network.

The QCM characterization result for the whole LbL assembly process of glucose sensor is shown in Fig. 4. It is clearly observed that the frequency decreases with the number of layers assembled, as shown in Fig. 4(a). The reason for the abrupt frequency increase corresponding to PDDA assembly after PSS, SWNT, and GOx is the viscosity of PDDA solution since frequency shift was collected in the solution not in the atmosphere. It assures exclusion of the effect of any moisture left after intermediate drying and contaminants adsorption from the atmosphere. The saturated frequency shifts are shown in Fig. 4(b). The average frequency shifts of either polycation like PDDA or polyanion such as PSS, SWNT, and GOx reveal the mass adsorbed on the surface in Sauerbrey equation, given by

$$\Delta f = -C_f \Delta m_s$$

where Δf is frequency shift in Hz, C_f sensitivity factor of the used crystal (0.181 $\mathrm{Hz} \cdot \mathrm{cm}^2 \cdot \mathrm{ng}^{-1}$ for the 9 MHz AT cut crystal), and Δm_s mass adsorbed per unit area in $\mathrm{ng/cm}^2$.

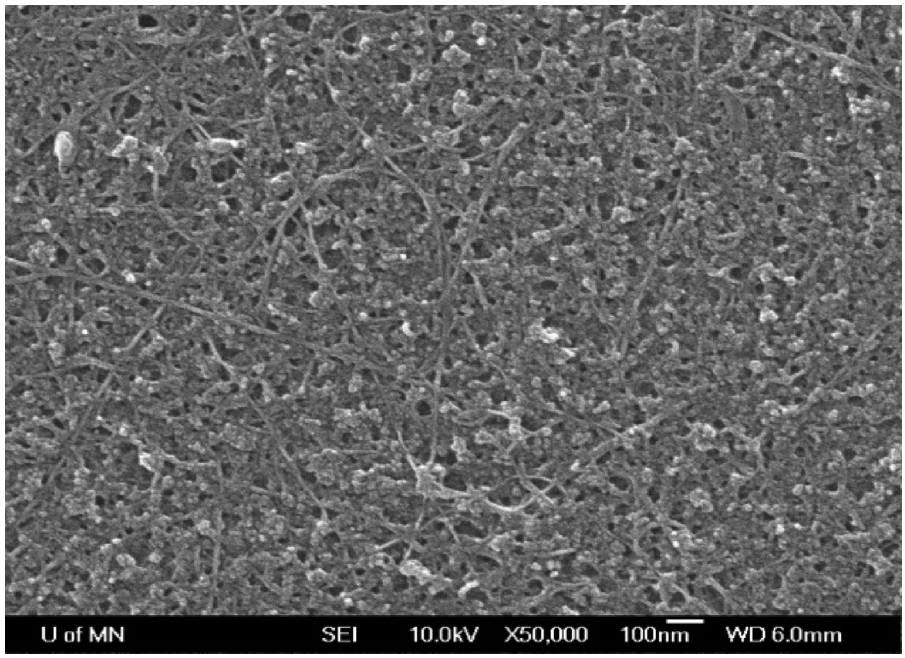

Fig. 3. Scanning electron microscopy (SEM) image of SWNT terminated surface. Individual SWNTs, bundles, and their random network are observed.

This is based on the fact that the crystal is fully covered with the materials assembly [25] and sustained by fully distributed SWNTs, as shown in Fig. 3. The averages of frequency shifts for (PDDA/PSS), (PDDA/SWNT), and (PDDA/GOx) bi-layers are 198, 299, and 65 Hz, respectively. In particular, the frequency decrease for (PDDA/SWNT) bi-layer is substantially consistent with the previous result [26]. The mass of assembled bi-layers, (PDDA/PSS), (PDDA/SWNT), and (PDDA/GOx) are calculated as 83, 125, and 27 ng, respectively. In addition, the thickness for each material can be calculated with the assumed density. The thicknesses for PDDA and SWNT are 2.8 and 4.8 nm, respectively [26]. Based on the assumed density, 1.3 $\mathrm{g/cm^3}$ [27], the bio-receptor thicknesses can be calculated as 2.8 nm under assumption that linear polyelectrolyte (PDDA) fully covers GOx, so that only GOx size is dominant. The smaller film thickness than actual diameter of GOx ($\sim 7\ \mathrm{nm}$) can be attributed to the sparse packing of GOx on the surface. From the QCM data, it is obvious that GOx is negatively charged, and multilayer can be built up alternatively with positively charged PDDA.

Complementary to QCM, FTIR was used to demonstrate GOx could be self-assembled onto the positively charged PDDA surfaces. The reflective FTIR spectra of PDDA, (PDDA/PSS), and $(\mathrm{PDDA/PSS})_2(\mathrm{PDDA/GOx})$ are shown in Fig. 5. Unlike the spectra of PDDA and (PDDA/PSS) control groups, the spectrum of GOx surface has several characteristic peaks. The strong absorption peak at 1664 $\mathrm{cm^{-1}}$ corresponds to $\mathrm{C=O}$ stretching vibration (amide I band, 1700–1600 $\mathrm{cm^{-1}}$) of peptide bonds of GOx backbone absorbed onto PDDA surface. Another strong peak at 1520 $\mathrm{cm^{-1}}$ results from N-H bending vibration (amide II band, 1600–1500 $\mathrm{cm^{-1}}$) of peptide bonds. Both strong peaks are in good agreement with reported results [28]. These two peaks are evident indications of the presence of GOx. Moreover, the weak peak at 3320 $\mathrm{cm^{-1}}$ is caused by N-H stretching of the peptide backbone, and peaks ranging from 1300–1240 $\mathrm{cm^{-1}}$ are attributed to amide band III [29]. In consequence, the absorption peaks found in the $(\mathrm{PDDA/PSS})_2(\mathrm{PDDA/GOx})$ compared to PDDA and (PDDA/PSS) ensure that enzyme GOx is negatively charged, and can be self-assembled alternatively with positively charged PDDA. Furthermore, FTIR is proven to be a potent tool to demonstrate the protein immobilized by LbL assembly, since it has been used for determination of protein secondary structure [29].

The electronic detection of pH responses is depicted in Fig. 6. The temporal responses of the conductance of $(\mathrm{PDDA/PSS})_2(\mathrm{PDDA/SWNT})_5$ device is shown in Fig. 6(a). In the atmosphere, the conductance was collected until it had been stabilized, and pH buffer solution was added. After the signal was stabilized in the buffer, the old buffer solution was removed and new buffer was added at the same time. The conductance of SWNT multilayer decreases exponentially, which had the time constant of 15 s. The inset shows the current after adding pH6 buffer solution and its curve fitting to exponential decaying function. Therefore, 1 min after adding the sample solution was allowed for the stabilization of signals in the following detection using parameter analyzer. In Fig. 6(b), I-V characteristics at different pH buffer are shown. It is noted that the current flowing through SWNT multilayer decreases with increase in pH at the same bias voltage. Replotting into current versus pH tells us that the current exponentially decreases as pH increases, which is well adapted to exponential function, as shown in Fig. 6(c). The effect of the ionic conductor due to buffer solutions used is negligible for transferring charge carriers at the low bias voltage. For this reason, hydrogen ions play a key role in changing the conductance of SWNT multi-

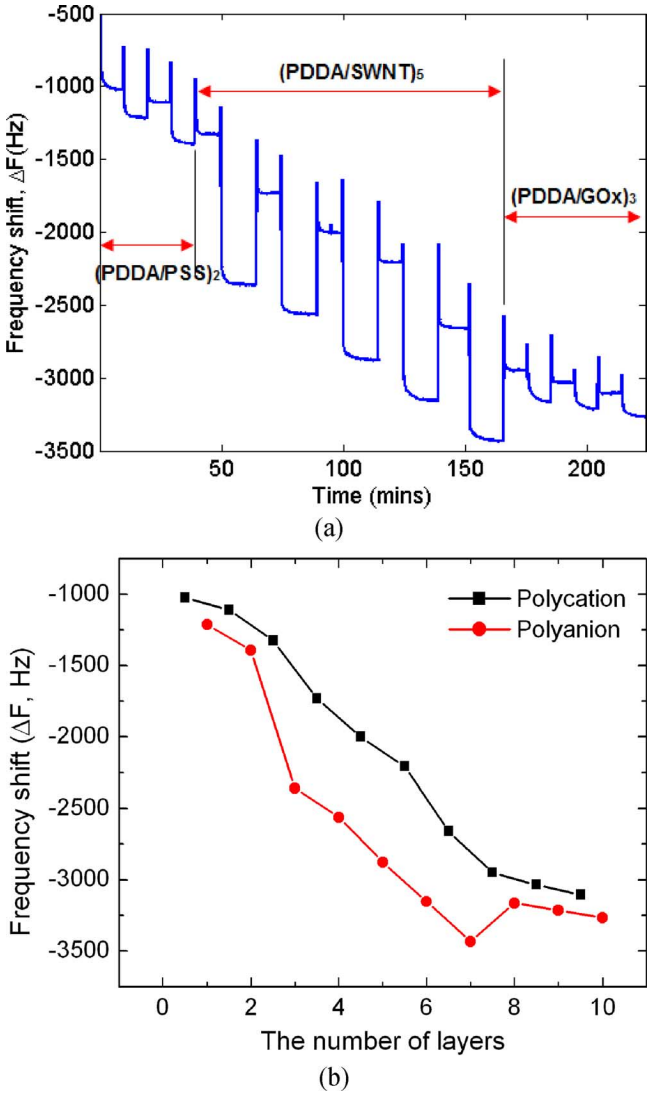

Fig. 4. QCM study of multilayer growth process of SWNT as an electrochemical transducer and GOx as a bio-receptor to fabricate the glucose sensors: (a) real-time monitoring of the frequency decrease of the crystal by adsorption and (b) the saturated frequency shift of polycation (PDDA) and polyanion (PSS, SWNT, and GOx).

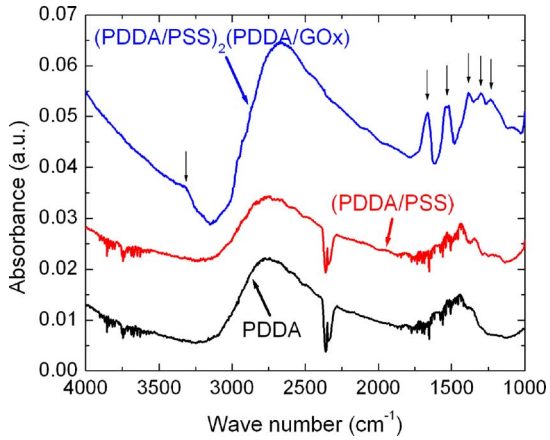

Fig. 5. Reflective FTIR spectra of PDDA, (PDDA/PSS), and $(\mathrm{PDDA/PSS})_2(\mathrm{PDDA/GOx})$ surfaces: Arrows indicate the presence of amide bonds in GOx.

layer assuming the same effects of other ions. In particular, the conductance of SWNT multilayer is believed to have something to do with protonation/deprotonation of carboxylic group in SWNTs as Henderson–Hasselbach equation implies, under the assumption that the acidities of all carboxylic groups in SWNTs are the same. The protonation/deprotonation in carboxylated SWNTs might be explained as the hole doping/undoping of semiconducting SWNTs from the conventional semiconductor perspectives [30], because carboxylated and LbL assembled CNTs have been proven to be p-type semiconductor [31].

The glucose testing of LbL assembled devices is shown in Fig. 7. All data of current versus glucose concentration were collected using the semiconductor parameter analyzer. First of all, $(\mathrm{PDDA/PSS})_2$ $(\mathrm{PDDA/SWNT})_5$ and $(\mathrm{PDDA/PSS})_2$ $(\mathrm{PDDA/GOx})_3$ has been chosen as control groups in the absence of the bio-receptor and transducer, respectively, in order to demonstrate that the combination of SWNT and GOx shows the capabilities of glucose sensing. The currents are depicted in Fig. 7(a) at a bias voltage of 0.6 V. The current in $(\mathrm{PDDA/PSS})_2$ $(\mathrm{PDDA/GOx})_3$ is almost constant at zero compared to other two groups, indicating that other salt ions do not play a significant role of transferring charge carriers between source and drain electrodes. On the other hand, the current in devices with only SWNT multilayer diminishes almost linearly with the increase of glucose concentration presumably due to the adsorption of glucose molecules onto SWNT surface and/or changes of the proximal ionic environment. Contrary to these, it is explicitly observed that the cooperation of SWNT and GOx shows the augmenting current with glucose concentration as previous discussions described elsewhere, as shown below [21], [23]

$$\beta - \mathrm{D} - \mathrm{glucose} + \mathrm{O_2} \xrightarrow{\mathrm{GOx}}$$
$$\mathrm{D} - \mathrm{glucono} - \delta - \mathrm{lactone} + \mathrm{H_2O_2}$$
$$\mathrm{D-glucono-}\,\delta\,\mathrm{-lactone} + \mathrm{H_2O} \rightarrow \mathrm{D} - \mathrm{gluconate}^{-} + \mathrm{H}^{+}.$$

β-D-glucose is oxidized to D-glucono-δ-lactone with the aid of GOx, followed by the hydrolysis to produce hydrogen ions. Based on the pH-dependent conductance changes in SWNT multilayer, the current flowing through the multilayer is dependent on glucose concentrations. Even though the pH in the bulk solution maintains relatively constant owing to buffering power of PBS, the local pH changes near GOx leads to protonation/deprotonation of carboxylic groups on SWNTs causing the conductance variation. Moreover, the effect of bias voltage on the current is shown in Fig. 7(b). As driving voltage increases, the current increases. It is expected that the sensitivity increases with glucose concentration at the constant bias voltage. However, it is worthy of mentioning that the sensitivity in the glucose sensing decreases with glucose concentration, as shown in Fig. 7(c), which is opposed to pH-responsive conductance behavior in Fig. 6(b). The decreasing sensitivity is caused by the enzyme GOx kinetics since the current corresponds to the rate of reaction and it is obviously enzyme limited, which has been proven in QCM results. The overall sensitivity upon

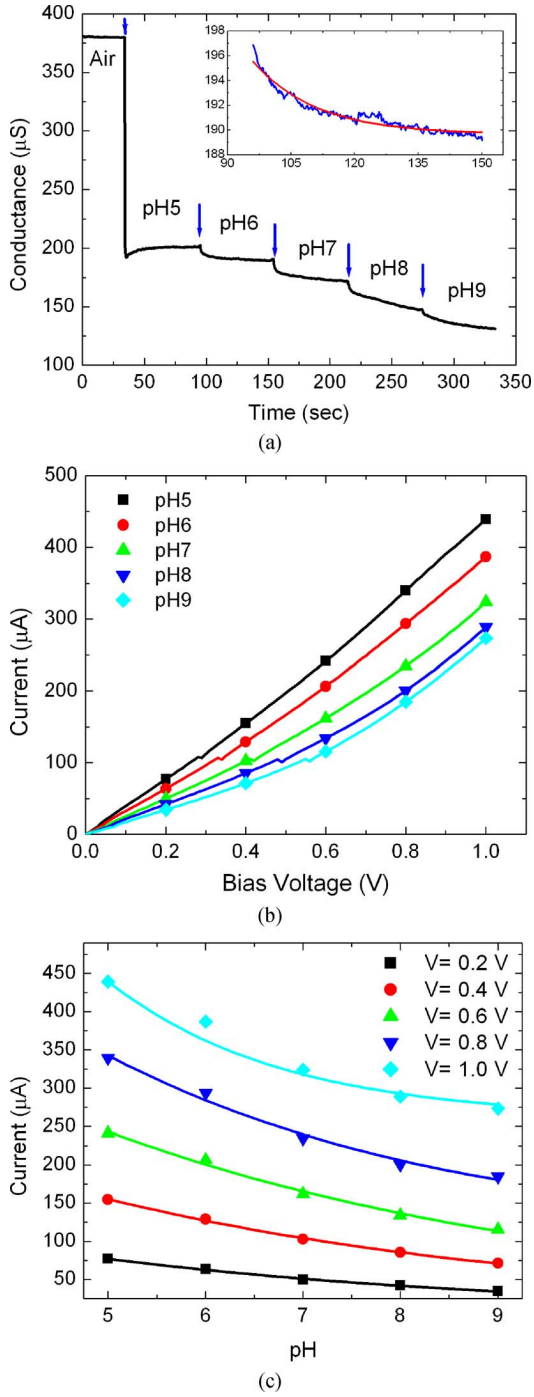

Fig. 6. pH-responsive electrical behaviors of SWNT multilayer, $(\mathrm{PDDA/PSS})_2$ $(\mathrm{PDDA/SWNT})_5$: (a) time responses at different buffer solutions, (b) I-V characteristics measured by parameter analyzer, and (c) replotting of (b) into current versus pH.

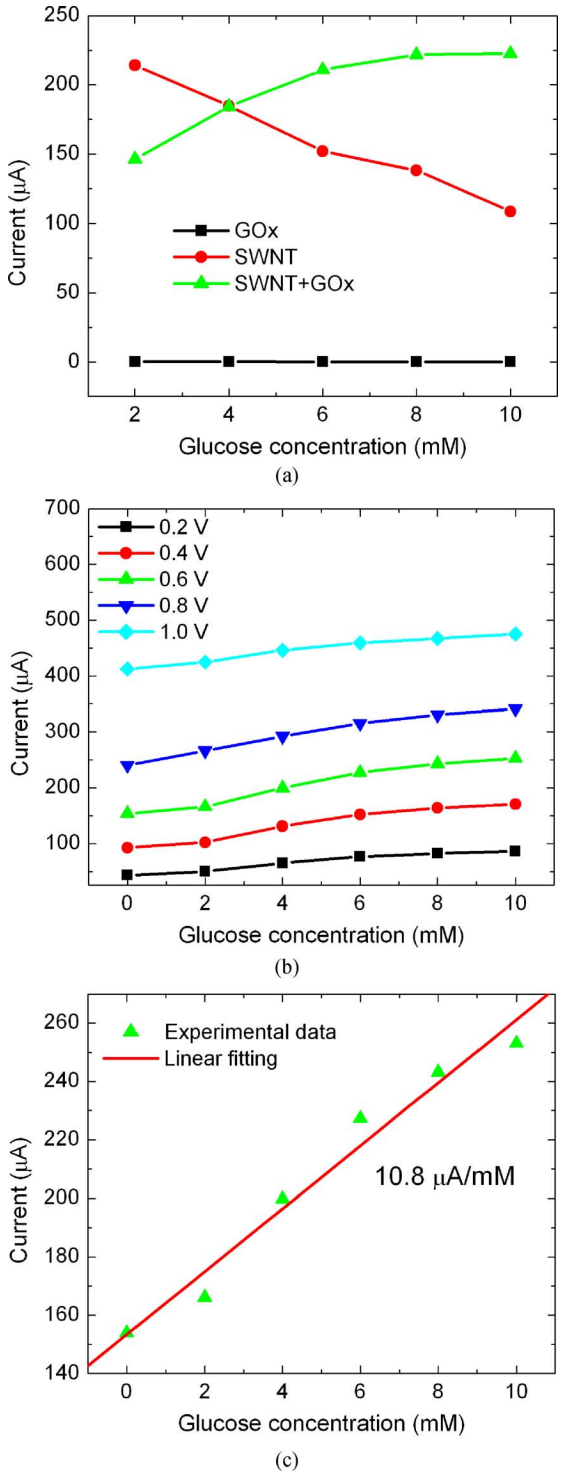

Fig. 7. Glucose concentration test of the fabricated sensor: (a) sensing capability of the combination of SWNT and GOx multilayer, (b) current versus glucose concentration at the various bias voltages, and (c) linear curve fitting to current data at the bias voltage of 0.6 V.

linear fitting has been found as 10.8 $\mu\mathrm{A/mM}$ at the bias voltage of 0.6 V. The sensitivity found in this study is remarkable compared to other planar devices reported previously [23], [32], [33] due to the highly sensitive SWNTs. The resolution of device fabricated is shown in Fig. 8 at the bias voltage of 0.6 V. Even though it shows a different current level and scale from the ones in Fig. 7, which was measured in the different chip, it is observed that the device can detect down to 1 pM glucose concentration presumably due to highly sensitive SWNTs. In addition, the result for the stability test is shown in Fig. 9. The device was stored in the refrigerator at 4 °C. The decreased overall sensitivity from 9.5 to 8.6 $\mu\mathrm{A/mM}$ is observed due to decreased enzyme activity, but the current level is increased 15

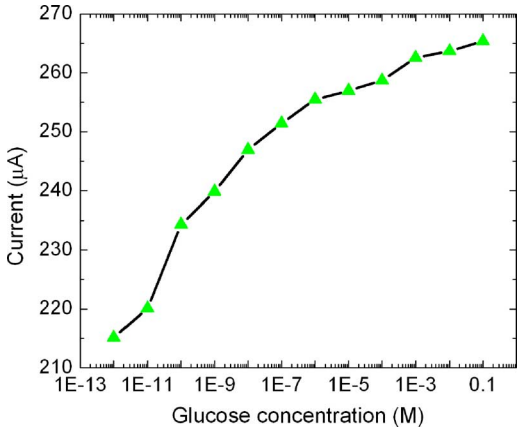

Fig. 8. Resolution test of the fabricated glucose sensor at the voltage of 0.6 V.

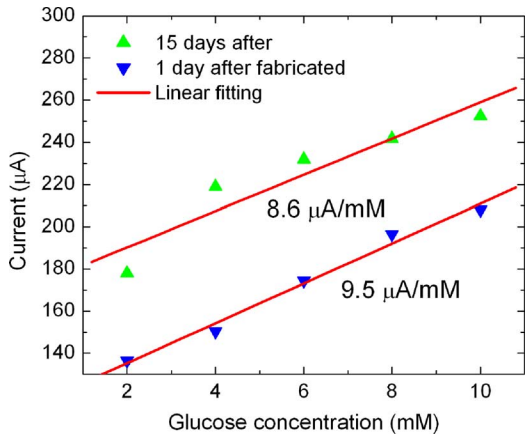

Fig. 9. Stability test of the fabricated glucose sensor stored in dry state at 4 °C.

days after fabrication presumably due to surface adsorption of the atmospheric particles or surface oxidation.

IV. Conclusion

We have fabricated the conductometric glucose sensors using LbL assembled SWNT and GOx. The GOx has been proven to be charged negatively and assembled successively using LbL technique as shown in FTIR and QCM results. LbL assembled thin-film SWNT multilayer shows exponential pH-dependent conductance by protonation/deprotonation of carboxylic functional groups on the SWNTs. Hydrogen ions penetrate into SWNT multilayer and have influence on its electronic conductance. Based on conductance change caused by pH change, glucose concentration can be detected by the local pH changes, which is caused basically by the oxidation of glucose catalyzed by GOx. The overall sensitivity and the resolution of device fabricated are 10.8 $\mu\mathrm{A}/\mathrm{mM}$ and 1 pM, respectively, at the bias voltage of 0.6 V. LbL assembled SWNT thin-film multilayer may detects many other biochemical reactions accompanied by pH change assisted by enzymatic reactions.

Acknowledgment

The authors acknowledge the Nanofabrication Center and Characterization Facility at the University of Minnesota for the help with fabrication and characterization.

References

[1] S. Iijima, "Helical microtubules of graphitic carbon," *Nature*, vol. 354, pp. 56–58, Nov. 1991.

[2] J. Han, "Structures and properties of carbon nanotubes," in *Carbon Nanotubes: Science and Applications*, M. Meyyappan, Ed., 1st ed. New York: CRC Press, 2005, pp. 8–24.

[3] E. S. Snow, F. K. Perkins, E. J. Houser, S. C. Badescu, and T. L. Reinecke, "Chemical detection with a single-walled carbon nanotube capacitor," *Science*, vol. 307, no. 5717, pp. 1942–1945, Mar. 2005.

[4] S. Sotiropoulou and N. A. Chaniotakis, "Carbon nanotube array-based biosensor," *Anal. Bioanal. Chem.*, vol. 375, no. 1, pp. 103–105, Jan. 2003.

[5] A. M. Fennimore, T. D. Yuzvinsky, W.-Q. Han, M. S. Fuhrer, J. Cumings, and A. Zettl, "Rotational actuators based on carbon nanotubes," *Nature*, vol. 424, pp. 408–410, Jul. 2003.

[6] Z. Chen, J. Appenzeller, Y.-M. Lin, J. Sippel-Oakley, A. G. Rinzler, J. Tang, S. J. Wind, P. M. Solomon, and P. Avouris, "An integrated logic circuit assembled on a single carbon nanotube," *Science*, vol. 311, no. 5768, p. 1735, Mar. 2006.

[7] C. Hierold, A. Jungen, C. Stampfer, and T. Helbling, "Nano electromechanical sensors based on carbon nanotubes," *Sens. Actuator A-Phys.*, vol. 136, no. 1, pp. 51–61, May 2007.

[8] M. Zhao, V. Sharma, H. Wei, R. R. Birge, J. A. Stuart, F. Papadimitrakopoulos, and B. D. Huey, "Ultrasharp and high aspect ratio carbon nanotube atomic force microscopy probes for enhanced surface potential imaging," *Nanotechnology*, vol. 19, no. 23, p. 235704, May 2008.

[9] K. Gong, Y. Yan, M. Zhang, L. Su, S. Xiong, and L. Mao, "Electrochemistry and electroanalytical applications of carbon nanotubes: A review," *Anal. Sci.*, vol. 21, no. 12, pp. 1383–1393, Dec. 2005.

[10] A. Star, J.-C. P. Gabriel, K. Bradley, and G. Grüner, "Electronic detection of specific protein binding using nanotube FET devices," *Nano. Lett.*, vol. 3, no. 4, pp. 459–463, 2003.

[11] X. Tang, S. Bansaruntip, N. Nakayama, E. Yenilmez, Y.-L. Chang, and Q. Wang, "Carbon nanotube DNA sensor and sensing mechanism," *Nano Lett.*, vol. 6, no. 8, pp. 1632–1636, 2006.

[12] M. Lu, D. Lee, W. Xue, and T. Cui, "Flexible and disposable immunosenosors based on layer-by-layer self-assembled carbon nanotubes and biomolcules," in *Proc. 21st IEEE Int. Conf. Micro Electro Mech. Syst.*, 2008, pp. 188–191.

[13] H. Boo, R.-A. Jeong, S. Park, K. S. Kim, K. H. An, Y. H. Lee, J. H. Han, H. C. Kim, and T. D. Chung, "Electrochemical nanoneedle biosensor based on multiwall carbon nanotube," *Anal. Chem.*, vol. 78, no. 2, pp. 617–620, Dec. 2006.

[14] J. Wang, M. Li, Z. Shi, N. Li, and Z. Gu, "Direct electrochemistry of cytochrome C at a glassy carbon electrode modified with single-wall carbon nanotubes," *Anal. Chem.*, vol. 74, no. 9, pp. 1993–1997, Mar. 2002.

[15] S. G. Wang, Q. Zhang, R. Wang, and S. F. Yoon, "A novel multi-walled carbon nanotube-based biosensor for glucose detection," *Biochem. Biophys. Res. Commun.*, vol. 311, no. 3, pp. 572–576, Nov. 2003.

[16] X. Chu, D. Duan, G. Shen, and R. Yu, "Amperometric glucose biosensor based on electrodeposition of platinum nanoparticles onto covalently immobilized carbon nanotube electrode," *Talanta*, vol. 71, no. 5, pp. 2040–2047, 2007.

[17] Y.-C. Tsai, S.-C. Li, and S.-W. Liao, "Electrodeposition of polypyrrole-multiwalled carbon nanotube-glucose oxidase nanobiocomposite film for the detection of glucose," *Biosens. Bioelectron.*, vol. 22, no. 4, pp. 495–500, Oct. 2006.

[18] X. B. Yan, X. J. Chen, B. K. Tay, and K. A. Khor, "Transparent and flexible glucose biosensor via layer-by-layer assembly of multi-wall carbon nanotubes and glucose oxidase," *Electrochem. Comm.*, vol. 9, no. 6, pp. 1269–1275, Jun. 2007.

[19] B.-Y. Wu, S.-H. Hou, F. Yin, Z.-X. Zhao, Y.-Y. Wang, X.-S. Wang, and Q. Chen, "Amperometric glucose biosensor based on multilayer films via layer-by-layer self-assembly of multi-wall carbon nanotubes, gold nanoparticles and glucose oxidase on the Pt electrode," *Biosens. Bioelectron.*, vol. 22, no. 12, pp. 2854–2860, Jun. 2007.

[20] Y. Zou, C. Xiang, L. Suna, and F. Xua, "Amperometric glucose biosensor prepared with biocompatible material and carbon nanotube by layer-by-layer self-assembly technique," *Electrochimica Acta*, vol. 53, no. 12, pp. 4089–4095, May 2008.

[21] X.-L. Luo, J.-J. Xu, W. Zhao, and H.-Y. Chen, "Glucose biosensor based on ENFET doped with SiO_2 nanoparticles," *Sens. Actuator B-Chem.*, vol. 97, no. 2-3, pp. 249–255, Feb. 2004.

[22] X.-L. Luo, J.-J. Xu, W. Zhao, and H.-Y. Chen, "A novel glucose ENFET based on the special reactivity of MnO_2 nanoparticles," *Biosens. Bioelectron.*, vol. 19, no. 10, pp. 1295–1300, May 2004.
[23] Y. Liu and T. Cui, "Glucose biosensors based on layer-by-layer nano self-assembled ion-sensitive field-effect transistors," *Sensor Lett.*, vol. 4, no. 3, pp. 241–245, Sep. 2006.
[24] F. Ricci, D. Moscone, C. S. Tuta, G. Palleschi, A. Amine, A. Poscia, F. Valgimigli, and D. Messeri, "Novel planar glucose biosensors for continuous monitoring use," *Biosens. Bioelectron.*, vol. 20, no. 10, pp. 1993–2000, Apr. 2005.
[25] M. Zhang, K. Gong, H. Zhang, and L. Mao, "Layer-by-layer assembled carbon nanotubes for selective determination of dopamine in the presence of ascorbic acid," *Biosens. Bioelectron.*, vol. 20, no. 7, pp. 1270–1276, 2005.
[26] W. Xue and T. Cui, "Characterization of layer-by-layer self-assembled carbon nanotube multilayer thin films," *Nanotechnology*, vol. 18, no. 14, p. 145709, Mar. 2007.
[27] Y. Lvov, K. Ariga, I. Ichinose, and T. Kunitake, "Assembly of multicomponent protein films by means of electrostatic layer-by-layer adsorption," *J. Amer. Chem. Soc.*, vol. 117, no. 22, pp. 6117–6123, 1995.
[28] W. Liang and Y. Zhuobin, "Direct electrochemistry of glucose oxidase at a gold electrode modified with single-wall carbon nanotubes," *Sensors*, vol. 3, no. 12, pp. 544–554, Dec. 2003.
[29] J. Grdadolnik, "Saturation effects in FTIR spectroscopy: Intensity of amide I and amide II bans in protein sepectra," *Acta Chim. Slov.*, vol. 50, no. 4, pp. 777–788, 2003.
[30] D. Lee and T. Cui, "pH-dependent conductance behaviors of layer-by-layer self-assembled carboxylated carbon nanotube multilayer thin-film sensors," *J. Vac. Sci. Technol. B*, 2009, DOI: 10.1116/1.3002386, in press.
[31] W. Xue, Y. Liu, and T. Cui, "High-mobility transistors based on nano-assembled carbon nanotube semiconducting layer and SiO_2 nanoparticle dielectric layer," *Appl. Phys. Lett.*, vol. 89, no. 16, p. 163512, Oct. 2006.
[32] T. Matsumoto, M. Furusawa, H. Fujiwara, Y. Matsumoto, and N. Ito, "A micro-planar amperometric glucose sensor unsusceptible to interference species," *Sens. Actuat. B*, vol. 49, pp. 68–72, 1998.
[33] J. Zhu, Z. Zhu, Z. Lai, R. Wang, X. Guo, X. Wu, G. Zhang, Z. Zhang, Y. Wang, and Z. Chen, "Planar amperometric glucose sensor based on glucose oxidase immobilized by chitosan film on prussian blue layer," *Sensors*, vol. 2, pp. 127–136, 2002.

Dongjin Lee received the B.S. and M.S. degrees in mechanical engineering from Korea University, Seoul, Korea, in 2003 and 2005, respectively. He is currently working towards the Ph.D. degree at the Department of Mechanical Engineering, University of Minnesota, Minneapolis.

From 2004 to 2005, he worked as a Guest Researcher at the Nanoscale Metrology Group, National Institute of Standards and Technology (NIST), MD. His main research topics include micro/nano manufacturing, nanomaterial based sensors and actuators, chemical and biological sensors, micro- and nanoelectromechanical systems (M/NEMS), and general nanotechnology.

Tianhong Cui (SM'04) received then B.S. degree from Nanjing University of Aeronautics and Astronautics, Nanjing, China, in 1991, and the Ph.D. degree from the Chinese Academy of Sciences, Beijing, China, in 1995.

He is currently a Nelson Associate Professor of Mechanical Engineering at the University of Minnesota. From 1999 to 2003, he was an Assistant Professor of Electrical Engineering at Louisiana Technical University. Prior to that, he was a STA Fellow at the National Laboratory of Metrology, and served as a Postdoctoral Research Associate at the University of Minnesota and Tsinghua University. His current research interests include MEMS/NEMS, nanotechnology, and polymer electronics.

Prof. Cui is a member of ASME. He received research awards including the Nelson Endowed Chair Professorship from the University of Minnesota, the Research Foundation Award from Louisiana Tech University, the Alexander von Humboldt Award in Germany, and the STA and NEDO Fellowships in Japan.